GEORGIAN BIOMEDICAL NEWS

VOLUME 4. ISSUE 2. APRIL-JUNE 2026

Age-Dependent Myocardial Remodeling and Fibrotic Vulnerability in Rats Subjected to Resistance-Loaded Swimming

Nikoloz Vachadze[1], Ramaz Khetsuriani[1], Marina Pailodze[1], Manana Arabuli[1], Elene Shvangiradze[1], Tamar Sultanishvili[1], Maia Kharabadze[1], Anzor Gogiberidze[1,ID], Nino Pruidze[1,ID]

ABSTRACT

BACKGROUND. Aging is characterized by cardiomyocyte loss, extracellular matrix expansion, increased ventricular stiffness, and reduced stress reserve. Exercise can induce adaptive cardiac hypertrophy, but sustained high-intensity overload may also promote maladaptive remodeling and fibrosis. Rodent swimming models with external loading are widely used to intensify exercise demand, yet age-stratified structural responses of the myocardium remain insufficiently characterized.

OBJECTIVES. To evaluate age-related differences in functional and histopathological myocardial remodeling in rats subjected to resistance-loaded swimming.

METHODS. Twenty-one (n=21) male Wistar rats were stratified into juvenile (3–4 months), adult (12–13 months), and geriatric (18–19 months) cohorts, with 7 (n=7) animals per cohort. All animals underwent a 6-week swimming protocol with a tail load equal to 4% of body weight. Hearts were harvested 24 hours after the final session and examined histologically using hematoxylin-eosin and Masson trichrome staining. Two blinded observers performed systematic assessment of four left ventricular regions. Fibrosis was quantified as percentage collagen area using digital image analysis.

RESULTS. Resistance-loaded swimming induced distinct age-dependent patterns of myocardial remodeling. Juvenile rats exhibited mild vascular congestion with minimal fibrosis (mean collagen area: 1.9±0.8%). Adult rats displayed the most extensive injury, characterized by marked perivascular and interstitial fibrosis (mean collagen area: 7.8±2.1%) and multifocal cardiomyocyte necrosis. Geriatric rats showed dystrophic changes with moderate focal fibrosis (mean collagen area: 4.6±1.5%). Differences in fibrosis among age cohorts were statistically significant ($p<0.001$, one-way ANOVA).

CONCLUSIONS. In this rat model, resistance-loaded swimming induced age-dependent myocardial remodeling. Adult animals' physiological adaptation from maladaptive remodeling when interpreting cardiac responses to high-intensity exercise across the lifespan.

KEYWORDS. Aging; Cardiac Fibrosis; Cardiac Remodeling; Echocardiography; Left Ventricle; Rat Model; Resistance Exercise; Swimming.

DOI. 10.52340/GBMN.2026.01.01.172

BACKGROUND

Cardiac aging is characterized by myocyte loss, reactive hypertrophy, extracellular matrix expansion, and progressive increases in myocardial stiffness that predispose to impaired relaxation and later heart failure. [1-4] Exercise modifies this trajectory in a stimulus-dependent manner: endurance training may promote physiological remodeling, whereas chronic pressure overload and excessive mechanical stress are more strongly associated with fibrosis and pathological hypertrophy. [5]

Swimming models are frequently used in rats to study exercise-induced cardiovascular adaptation because exercise intensity can be increased by attaching a load to the tail, thereby converting free swimming into a higher-resistance protocol. [6-8] Prior animal studies have shown that swimming training can induce cardiac hypertrophy and alter ventricular geometry. [9-10]

The present study was designed to examine whether age modifies the balance between geometric adaptation and tissue injury during resistance-loaded swimming. We hypothesized that all exercise-exposed age groups would show evidence of myocardial remodeling, but that the structural cost of adaptation - particularly fibrosis - would vary across the lifespan.

METHODS

This study used 21 male Wistar rats, which are commonly used in swimming-based cardiovascular experiments. Animals were stratified into three age cohorts: juvenile (3–4 months), adult (12–13 months), and geriatric (18–19 months), with 7 rats per cohort. These age cutoffs were defined based on established

GEORGIAN BIOMEDICAL NEWS

VOLUME 4. ISSUE 2. APRIL-JUNE 2026

rodent cardiac aging literature. Juvenile rats (1–3 months correspond to young adults with preserved cardiomyocyte proliferative capacity and minimal baseline fibrosis. Adult rats represent mature animals at peak contractile performance with established extracellular matrix homeostasis but declining regenerative potential. Geriatric rats exhibit age-related fibrotic accumulation, increased myocardial stiffness, and reduced adaptive reserve. All animals underwent the same 6-week resistance-loaded swimming protocol. No sedentary control group was included, as the primary objective was to characterize age-dependent responses to a standardized overload stimulus rather than to compare exercise versus rest within each age group. Animals were housed in a conventional laboratory facility at 22±2°C with relative humidity maintained within the accepted mammalian laboratory range, under a 12:12-hour reversed light-dark cycle with the dark phase scheduled from 07:00 to 19:00 to match exercise timing. Standard pellet chow and water were provided "ad libitum", and animals were acclimatized for 7 days before the intervention. Experimental conduct and husbandry were aligned with the Guide for the Care and Use of Laboratory Animals and with ARRIVE 2.0 reporting principles. [11,12] Randomization to age cohorts was based on date of birth. No animals were excluded from the analysis, and no adverse events requiring early termination occurred during the study period.

Aquatic adaptation and resistance-loaded swimming

To reduce non-exercise stress, rats were acclimatized to shallow warm water during the week preceding training. Swimming was then performed individually in a cylindrical tank filled to a depth sufficient to prevent tail support, with water maintained at 30-32°C. Rats swam for 60 minutes daily, 7 days per week, for 6 weeks. A lead weight equal to 4% of each rat's body weight was attached to the proximal tail at the start of each session and adjusted weekly after weighing. The selected water temperature and duration were based on established rat swimming protocols. In contrast, the external load was chosen to create a resistance-dominant stimulus rather than free-swimming endurance alone. [6-8,13-15]

Tissue collection and histological processing

Twenty-four hours after the final training session, rats were deeply anesthetized with intraperitoneal sodium pentobarbital (60 mg/kg) and euthanized by exsanguination followed by thoracotomy. Hearts were rapidly excised, rinsed in cold phosphate-buffered saline, blotted dry, weighed, and fixed in 10% neutral buffered formalin for 24 to 48 hours.

Transverse left ventricular sections were obtained at three standardized levels: basal, mid-ventricular, and apical. Sections were paraffin-embedded, cut, and stained with hematoxylin-eosin (H&E) for cellular injury and vascular congestion, and with Masson trichrome for collagen deposition.

Microscopic examination was performed systematically across four left ventricular regions: the anterior wall, lateral wall, posterior wall, and interventricular septum. This systematic approach ensured that regional variation in injury burden was captured without post hoc selection bias.

Histopathological assessment

Two blinded observers evaluated all histological slides. Discrepancies in scoring were resolved by consensus review with a third observer.

For fibrosis quantification, five non-overlapping fields per region (20 fields per heart) were captured from Masson trichrome-stained sections at 200× magnification using a digital microscope camera. Collagen area fraction (percentage of blue-stained area relative to total myocardial tissue area) was calculated using ImageJ software with a standardized color thresholding protocol.

Cardiomyocyte injury was evaluated on H&E-stained sections and categorized semiquantitatively as: Grade 0 (none), Grade 1 (mild, scattered hypereosinophilic myocytes), Grade 2 (moderate, multifocal necrosis with inflammatory infiltrate), or Grade 3 (severe, confluent areas of necrosis). Vascular congestion was graded semiquantitatively as Grade 0 (absent), Grade 1 (mild), Grade 2 (moderate), or Grade 3 (severe) based on the degree of capillary and venous dilatation.

GEORGIAN BIOMEDICAL NEWS

VOLUME 4. ISSUE 2. APRIL-JUNE 2026

Statistical analysis

Data are presented as mean ± standard deviation (SD). Semiquantitative injury and congestion grades were compared using the Kruskal-Wallis test with Dunn's post-hoc correction. A two-sided p-value <0.05 was considered statistically significant. All analyses were performed using GraphPad Prism software (version 9.0).

RESULTS

All 21 animals completed the 6-week protocol without adverse events. Body weights and heart weights for each age cohort are summarized in **TABLE 1**. As expected, body weight increased progressively with age (p<0.001 across groups). Absolute heart weight was highest in geriatric rats (p<0.001 vs. juvenile). In contrast, the heart weight-to-body weight ratio was highest in juvenile rats (p<0.05 vs. adult and geriatric), consistent with the known age-related decline in relative cardiac mass.

TABLE 1. Morphometric data by age cohort

Parameter	Juvenile (n=7)	Adult (n=7)	Geriatric (n=7)	p-value
Baseline body weight (g)	215±18	468±32*	542±41*†	<0.001
Final body weight (g)	292±22	505±38*	568±45*†	<0.001
Heart weight (mg)	1015±95	1420±125*	1550±140*	<0.001
Heart weight to Body weight ratio(mg/g)	3.48±0.22	2.81±0.19*	2.73±0.18*	<0.001

Explanations: Data are presented as mean ± SD. *p<0.05 vs. Juvenile; †p<0.05 vs. Adult.

Histopathological findings

Juvenile cohort (3-4 months, n=7): Juvenile rats demonstrated a consistent pattern of mild vascular congestion, characterized by dilated capillaries and venules throughout the myocardium, most pronounced in the subendocardial region. H&E staining revealed scattered hypereosinophilic myocytes suggestive of early ischemic injury in 6 of 7 animals, but no frank necrosis was observed in any animal. Masson trichrome staining showed minimal collagen deposition (mean collagen area: 1.9±0.8%; range: 0.9-3.2%). The fibrosis was predominantly perivascular, with preservation of the interstitial architecture. Representative findings are shown in **FIGURE 1**.

FIGURE 1. Histopathological findings in juvenile cohort

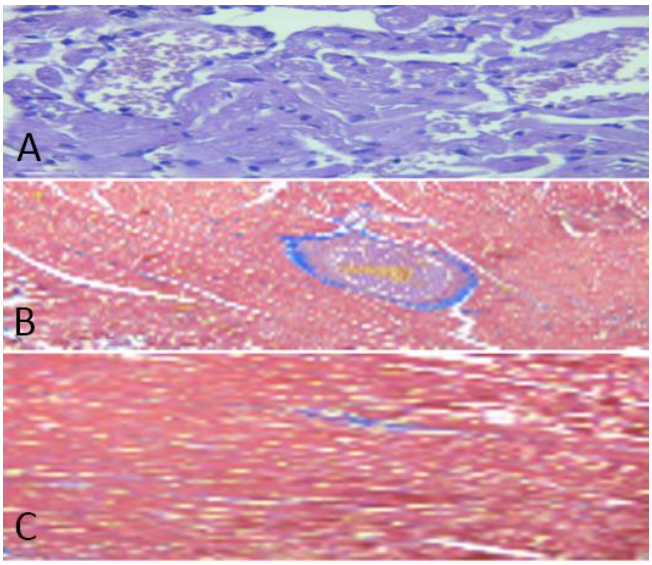

Explanations: Sample A - Juvenile cohort – H&E, anterior wall, showing mild vascular congestion. Representative section from the anterior left ventricular wall of a juvenile rat showing mild vascular congestion with dilated capillaries. No necrosis is observed. Sample B: Juvenile cohort – Masson trichrome, anterior wall, minimal perivascular collagen. Anterior left ventricular wall demonstrating minimal perivascular collagen deposition. Interstitial architecture is preserved. Sample C: Juvenile cohort – Masson trichrome, posterior wall, preserved architecture. Posterior left ventricular wall showing preserved myocardial architecture with negligible collagen deposition.

Adult cohort (12–13 months, n=7): Adult rats exhibited the most pronounced histopathological changes among all groups. H&E staining revealed moderate to severe venous congestion in all 7 animals and multifocal areas of cardiomyocyte necrosis in 6 of 7 animals. Necrotic foci were characterized by hypereosinophilic myocytes with loss of cross-striations, nuclear pyknosis, and associated inflammatory infiltrate. The anterior left ventricular wall was most severely affected, though injury extended to the lateral wall in 5 animals. Masson trichrome staining demonstrated prominent perivascular and interstitial fibrosis (mean collagen

GEORGIAN BIOMEDICAL NEWS

VOLUME 4. ISSUE 2. APRIL-JUNE 2026

area: 7.8±2.1%; range: 5.1–11.2%). Collagen deposition was most extensive surrounding intramyocardial vessels and extending into the adjacent interstitium, with associated myocyte disorganization and separation of fiber bundles. Fibrosis was significantly greater in adult rats compared to both juvenile ($p<0.001$) and geriatric ($p=0.008$) cohorts. Representative findings are shown in **FIGURE 2**.

FIGURE 2. Histopathological findings in adult cohort

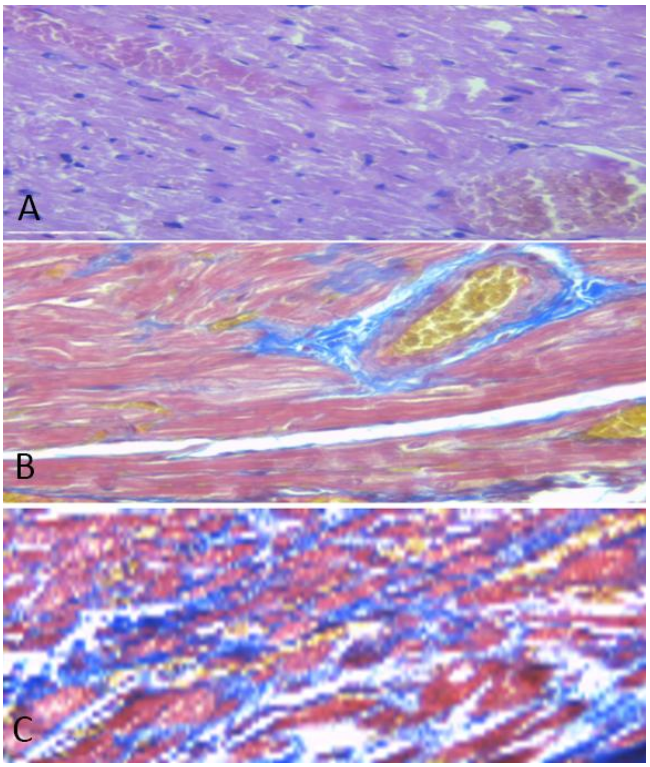

Explanations: Sample A: Adult cohort – H&E, anterior wall, showing necrosis and severe congestion. Anterior left ventricular wall demonstrating marked venous congestion and multifocal cardiomyocyte necrosis characterized by hypereosinophilic myocytes with nuclear pyknosis. Sample B: Adult cohort – Masson trichrome, anterior wall, marked perivascular fibrosis. Anterior left ventricular wall showing prominent perivascular fibrosis with dense collagen deposition surrounding intramyocardial vessels. Sample C: Adult cohort – Masson trichrome, lateral wall, diffuse interstitial expansion. Lateral left ventricular wall demonstrating diffuse interstitial fibrosis with separation of myocardial fibers by collagenous tissue.

Geriatric cohort (18–19 months, n=7): Geriatric rats showed dystrophic cardiomyocyte changes, including cytoplasmic vacuolization, irregular nuclear morphology, and scattered hypereosinophilic myocytes in all 7 animals. Vascular congestion was mild to moderate, less pronounced than in adult animals. Masson trichrome staining revealed moderate, focal fibrosis (mean collagen area: 4.6±1.5%; range: 2.8–6.9%). The fibrotic pattern was characterized by discrete patches of collagen deposition interspersed with areas of preserved myocardial architecture, in contrast to the more diffuse interstitial expansion observed in adult animals. Fibrosis was significantly lower in geriatric rats compared to adult rats ($p=0.008$), but remained significantly higher than in juvenile rats ($p=0.012$). Representative findings are shown in **FIGURE 3**.

FIGURE 3. Histopathological findings in geriatric cohort

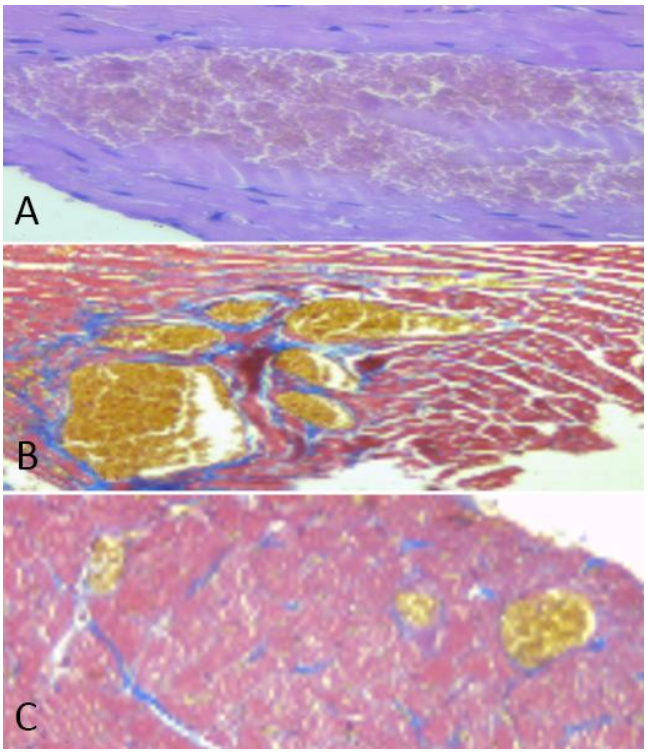

Explanations: Sample A: Geriatric cohort – H&E, anterior wall, dystrophic changes. Anterior left ventricular wall showing dystrophic cardiomyocyte changes including cytoplasmic vacuolization. Vascular congestion is mild. Sample B: Geriatric cohort – Masson trichrome, anterior wall, focal fibrosis. Anterior left ventricular wall demonstrating focal fibrosis with discrete patches of

collagen deposition. Sample C: Geriatric cohort – Masson trichrome, septal region, patchy collagen.

Interventricular septum showing patchy interstitial collagen deposition with overall preserved tissue architecture. Quantitative analysis of collagen area fraction confirmed significant differences in fibrotic burden across age cohorts.

DISCUSSION

This study demonstrates that resistance-loaded swimming induces age-dependent myocardial remodeling in rats, with adult animals exhibiting the most extensive histopathological injury and fibrosis. These findings provide insight into how myocardial biological age influences the structural response to sustained pressure overload.

The pattern observed in juvenile rats - vascular congestion with minimal fibrosis - is consistent with an acute hemodynamic stress response in myocardium that retains substantial structural resilience. Younger myocardium possesses greater cardiomyocyte proliferative capacity and more favorable extracellular matrix dynamics, which may account for the limited collagen deposition observed despite evidence of vascular congestion and early myocyte injury. [1,3] The mean collagen area of 1.9% in juvenile rats approximates values reported for healthy young rodent myocardium, suggesting that the 6-week overload did not trigger significant maladaptive remodeling in this age group.

Adult rats showed the most extensive histopathological changes, including necrosis and marked fibrosis. The mean collagen area of 7.8% represents a substantial increase above baseline values for this age group and falls within ranges associated with pathological remodeling in rodent models of pressure overload. This observation raises the possibility that adult myocardium represents a stage at which substantial contractile capacity coexists with reduced reparative flexibility. This pattern is consistent with the broader aging literature, which indicates that extracellular matrix turnover, inflammatory signaling, and fibrotic propensity change progressively across the life course. [2-4]

The pronounced response in adult animals may reflect a combination of high force-generating capacity (leading to greater mechanical stress during loaded swimming) and declining adaptive reserve relative to juvenile myocardium. Additionally, the adult heart may be at a transition point at which pro-fibrotic signaling pathways are more readily activated by biomechanical stress.

Geriatric rats displayed dystrophic changes and moderate focal fibrosis, which were significantly less extensive than in adult animals. This finding should not be interpreted as evidence that advanced age is protective. Rather, several factors may explain the attenuated fibrotic response. Geriatric rats may generate lower absolute force during swimming due to age-related sarcopenia and reduced exercise capacity, potentially resulting in a lower effective overload stimulus despite the standardized 4% tail load. Additionally, baseline age-related fibrosis may alter myocardial mechanical properties, thereby altering the pattern of stress distribution during exercise. Finally, the aged myocardium may exhibit a blunted capacity to mount a robust fibrotic response due to cellular senescence and altered signaling dynamics. [2]

Regional vulnerability of the anterior wall

The consistent finding that the anterior left ventricular wall exhibited the greatest injury burden across all age cohorts warrants consideration. The anterior wall is subjected to distinct mechanical forces during contraction, and in the rat heart, it lies adjacent to the sternum and rib cage. During the intense physical activity of loaded swimming, repetitive mechanical compression and elevated intrathoracic pressure may contribute to localized stress in this region. Similar regional vulnerability has been noted in other models of exercise-induced cardiac stress, though the precise mechanisms remain to be elucidated.

Implications for exercise prescription and cardiac health

These findings have potential translational implications. The observation that adult animals are most susceptible to exercise-induced fibrosis suggests that the middle-aged heart may be particularly vulnerable. This aligns with clinical observations that the benefits versus risks of high-intensity exercise may

shift across the lifespan. While exercise remains a cornerstone of cardiovascular health promotion, its intensity and modality may need to be tailored to an individual's biological age.

CONCLUSIONS

In this study, resistance-loaded swimming induced age-dependent myocardial remodeling in rats, characterized by distinct patterns of injury and fibrosis across juvenile, adult, and geriatric cohorts. Adult animals exhibited the most pronounced maladaptive remodeling, with extensive perivascular and interstitial fibrosis; juvenile animals showed minimal fibrosis despite evidence of hemodynamic stress; and geriatric animals displayed an intermediate, focal fibrotic response. These findings underscore the importance of considering biological age as a critical determinant of the cardiac response to high-intensity exercise.

AUTHOR AFFILIATION

1. Department of Human Anatomy, Tbilisi State Medical University, Tbilisi, Georgia.

SUPPLEMENTARY MATERIALS

N/A

ACKNOWLEDGEMENTS

This study received no specific grant from any funding agency in the public, commercial, or not-for-profit sectors.

The authors used Grammarly (V 1.2.208) solely to improve language clarity, grammar, spelling, tone, and readability during manuscript preparation. The tool was not used for data analysis, result interpretation, or the generation of scientific content. All scientific content, conclusions, and final wording were reviewed and approved by the authors.

REFERENCES

1. Anversa P, Palackal T, Sonnenblick EH, Olivetti G, Meggs LG, Capasso JM. Myocyte cell loss and myocyte cellular hyperplasia in the hypertrophied aging rat heart. Circ Res. 1990;67(4):871-885. doi:10.1161/01.RES.67.4.871.
2. Biernacka A, Frangogiannis NG. Aging and cardiac fibrosis. Aging Dis. 2011;2(2):158-173.
3. Lakatta EG, Levy D. Arterial and cardiac aging: major shareholders in cardiovascular disease enterprises: part II: the aging heart in health: links to heart disease. Circulation. 2003;107(2):346-354. doi:10.1161/01.CIR.0000048893.62841.F7.
4. Weber KT, Brilla CG. Pathological hypertrophy and cardiac interstitium: fibrosis and the renin-angiotensin-aldosterone system. Circulation. 1991;83(6):1849-1865. doi:10.1161/01.CIR.83.6.1849.
5. McMullen JR, Jennings GL. Differences between pathological and physiological cardiac hypertrophy: novel therapeutic strategies to treat heart failure. Clin Exp Pharmacol Physiol. 2007;34(4):255-262. doi:10.1111/j.1440-1681.2007.04585.x.
6. Geenen DL, Buttrick PM, Scheuer J. Cardiovascular adaptations to swimming training in the rat. J Appl Physiol (1985). 1988;65(3):1163-1168. doi:10.1152/jappl.1988.65.3.1163.
7. Schaible TF, Scheuer J. Effects of physical training by swimming on cardiac performance of the rat. J Appl Physiol Respir Environ Exerc Physiol. 1979;46(4):854-860. doi:10.1152/jappl.1979.46.4.854.
8. Evangelista FS, Brum PC, Krieger JE. Duration-controlled swimming exercise training induces cardiac hypertrophy in mice. J Appl Physiol (1985). 2003;95(2):617-624. doi:10.1152/japplphysiol.00373.2002.
9. Ribeiro S, Pereira ARS, Pinto AT, et al. Echocardiographic assessment of cardiac anatomy and function in adult rats. J Vis Exp. 2019;(154):e60404. doi:10.3791/60404.
10. Van der Veen BJ, de Boer RA, van der Velden J, et al. Towards standardization of echocardiography for the evaluation of left ventricular function in adult rodents: a position paper of the ESC Working Group on Myocardial Function. Cardiovasc Res. 2021;117(1):43-59. doi:10.1093/cvr/cvaa110.
11. National Research Council. Guide for the Care and Use of Laboratory Animals. 8th ed. National Academies Press; 2011. doi:10.17226/12910.
12. Percie du Sert N, Hurst V, Ahluwalia A, et al. The ARRIVE guidelines 2.0: updated guidelines for reporting animal research. PLoS Biol. 2020;18(7):e3000410. doi:10.1371/journal.pbio.3000410.
13. Hohl R, de Oliveira RB, Ferraresso RLP, Brenzikofer R, Macedo DV. Effect of body weight variation on swimming exercise workload in rats with constant and size-adjusted loads. Scand J Lab Anim Sci. 2011;38(3):145-154.
14. Gonçalves IO, Maciel E, Passos E, et al. Swimming training induces liver mitochondrial adaptations to oxidative stress in rats submitted to repeated

exhaustive swimming bouts. PLoS One. 2013;8(2):e55668. doi:10.1371/journal.pone.0055668.

15. de Andrade AGP, de Souza VA, da Silva VRR, et al. Sex differences in morphological and functional aspects of exercise-induced cardiac hypertrophy in rats. Front Physiol. 2019;10:889. doi:10.3389/fphys.2019.00889.